

NASA/TM—2012-217607

GT2011-46390



Comparison of Various Supersonic Turbine Tip Designs to Minimize Aerodynamic Loss and Tip Heating

Vikram Shyam
Glenn Research Center, Cleveland, Ohio

Ali Ameri
The Ohio State University, Columbus, Ohio

NASA STI Program . . . in Profile

Since its founding, NASA has been dedicated to the advancement of aeronautics and space science. The NASA Scientific and Technical Information (STI) program plays a key part in helping NASA maintain this important role.

The NASA STI Program operates under the auspices of the Agency Chief Information Officer. It collects, organizes, provides for archiving, and disseminates NASA's STI. The NASA STI program provides access to the NASA Aeronautics and Space Database and its public interface, the NASA Technical Reports Server, thus providing one of the largest collections of aeronautical and space science STI in the world. Results are published in both non-NASA channels and by NASA in the NASA STI Report Series, which includes the following report types:

- **TECHNICAL PUBLICATION.** Reports of completed research or a major significant phase of research that present the results of NASA programs and include extensive data or theoretical analysis. Includes compilations of significant scientific and technical data and information deemed to be of continuing reference value. NASA counterpart of peer-reviewed formal professional papers but has less stringent limitations on manuscript length and extent of graphic presentations.
- **TECHNICAL MEMORANDUM.** Scientific and technical findings that are preliminary or of specialized interest, e.g., quick release reports, working papers, and bibliographies that contain minimal annotation. Does not contain extensive analysis.
- **CONTRACTOR REPORT.** Scientific and technical findings by NASA-sponsored contractors and grantees.

- **CONFERENCE PUBLICATION.** Collected papers from scientific and technical conferences, symposia, seminars, or other meetings sponsored or cosponsored by NASA.
- **SPECIAL PUBLICATION.** Scientific, technical, or historical information from NASA programs, projects, and missions, often concerned with subjects having substantial public interest.
- **TECHNICAL TRANSLATION.** English-language translations of foreign scientific and technical material pertinent to NASA's mission.

Specialized services also include creating custom thesauri, building customized databases, organizing and publishing research results.

For more information about the NASA STI program, see the following:

- Access the NASA STI program home page at <http://www.sti.nasa.gov>
- E-mail your question to help@sti.nasa.gov
- Fax your question to the NASA STI Information Desk at 443-757-5803
- Phone the NASA STI Information Desk at 443-757-5802
- Write to:
STI Information Desk
NASA Center for AeroSpace Information
7115 Standard Drive
Hanover, MD 21076-1320



Comparison of Various Supersonic Turbine Tip Designs to Minimize Aerodynamic Loss and Tip Heating

Vikram Shyam
Glenn Research Center, Cleveland, Ohio

Ali Ameri
The Ohio State University, Columbus, Ohio

Prepared for the
TURBO EXPO 2011
sponsored by the American Society of Mechanical Engineers (ASME)
Vancouver, British Columbia, Canada, June 6–10, 2011

National Aeronautics and
Space Administration

Glenn Research Center
Cleveland, Ohio 44135

Acknowledgments

This work was supported by the Fundamental Subsonic Fixed Wing program at the NASA Glenn Research Center and addresses the milestone SFW.11.02.003—Develop and validate unsteady Reynolds Averaged Navier Stokes (RANS) and Large Eddy Simulations (LES) methods for engine flows. We would like to acknowledge the support of Dr. David L. Rigby, Arctic Slope Research Company (ASRC), who works at the NASA Glenn Research Center.

Trade names and trademarks are used in this report for identification only. Their usage does not constitute an official endorsement, either expressed or implied, by the National Aeronautics and Space Administration.

This work was sponsored by the Fundamental Aeronautics Program at the NASA Glenn Research Center.

Level of Review: This material has been technically reviewed by technical management.

Available from

NASA Center for Aerospace Information
7115 Standard Drive
Hanover, MD 21076–1320

National Technical Information Service
5301 Shawnee Road
Alexandria, VA 22312

Available electronically at <http://www.sti.nasa.gov>

Comparison of Various Supersonic Turbine Tip Designs to Minimize Aerodynamic Loss and Tip Heating

Vikram Shyam
National Aeronautics and Space Administration
Glenn Research Center
Cleveland, Ohio 44130

Ali Ameri
The Ohio State University
Columbus, Ohio 43210

Abstract

The rotor tips of axial turbines experience high heat flux and are the cause of aerodynamic losses due to tip clearance flows, and in the case of supersonic tips, shocks. As stage loadings increase, the flow in the tip gap approaches and exceeds sonic conditions. This introduces effects such as shock-boundary layer interactions and choked flow that are not observed for subsonic tip flows that have been studied extensively in literature. This work simulates the tip clearance flow for a flat tip, a diverging tip gap and several contoured tips to assess the possibility of minimizing tip heat flux while maintaining a constant massflow from the pressure side to the suction side of the rotor, through the tip clearance. The Computational Fluid Dynamics (CFD) code GlennHT was used for the simulations. Due to the strong favorable pressure gradients the simulations assumed laminar conditions in the tip gap. The nominal tip gap width to height ratio for this study is 6.0. The Reynolds number of the flow is 2.4×10^5 based on nominal tip width and exit velocity. A wavy wall design was found to reduce heat flux by 5 percent but suffered from an additional 6 percent in aerodynamic loss coefficient. Conventional tip recesses are found to perform far worse than a flat tip due to severe shock heating. Overall, the baseline flat tip was the second best performer. A diverging converging tip gap with a hole was found to be the best choice. Average tip heat flux was reduced by 37 percent and aerodynamic losses were cut by over 6 percent.

Nomenclature

δ	separation bubble height
h	tip gap height
h_x	heat transfer coefficient
k	thermal conductivity
M	Mach number
Nu	Nusselt number, h_x/k
P	pressure
w	tip width

x	distance along tip, with $x = 0.0$ at the pressure side edge
Y	aerodynamic loss coefficient

Subscripts:

0	total or stagnation conditions
1	at inlet to tip gap
2	at exit from tip gap

Introduction

A significant concern in turbine rotors is aerodynamic loss due to tip leakage. The pressure distribution set up around the rotor blade results in a pressure gradient across the tip gap of the rotor. The high pressure gas on the pressure side of the blade has a tendency to flow towards the suction side, which is at a lower pressure, across the tip. The path of the tip flow depends on several parameters such as blade rotational rate, blade geometry (tapering, twist, camber, tip gap height, and tip contouring) and flow inlet angle. These parameters can be reduced to the ratio of tip width to tip gap height, tip inlet Mach number and flow direction. No matter what the cause of the leakage flow, it results in a drop in efficiency and aerodynamic loss.

A detailed literature review of the basic features of turbine tip flow and heat transfer has been conducted by Bunker (Ref. 1) and Glezer et al. (Ref. 2). Glezer et al. (Ref. 2) describe the primary flow features seen due to tip leakage: the pressure side separation bubble on the tip surface and the tip leakage vortex. The extent of the bubble and its reattachment are contingent on blade thickness, Mach number, Reynolds number and tip height (Refs. 2 and 3). For subsonic flows, the percentage of inlet flow that constitutes the tip leakage is shown to grow linearly with tip gap height. In both References 1 and 2 the importance of Computational Fluid Dynamics (CFD) in tip flow and heat transfer prediction is emphasized especially due to the difficulty of conducting experimental measurements in a rotating tip gap. O'Dowd et al. (Ref. 4) used several techniques to measure the heat transfer coefficient and adiabatic wall temperature on a transonic

turbine blade tip (Rolls Royce Environmentally Friendly Engine). The complexity of measuring accurately the heat flux in the tip gap is elaborated on and it is for this reason that CFD is of great benefit. Ameri et al. (Ref. 5) simulated the GE-EEE (Energy Efficient Engine) high pressure turbine stage and studied the tip flow and heat transfer for a smooth tip and for a recessed tip. The cavity height of the recess was varied in the study to analyze the effect of recess depth on tip heat transfer. Two primary vortex structures were observed in the recess. It was found that the recess had negligible effect on loss and did not improve the heat transfer distribution on the tip as a whole. Another study by Ameri et al. (Ref. 6) investigated the effect of upstream casing recess on tip leakage and heat transfer and found that minimal tip heat transfer occurred for a recess height that is almost equal to tip clearance. They concluded that the recess has little effect on efficiency. This can be explained by approximating the effective tip gap geometry by a diverging-converging nozzle. Unless the tip gap height is extremely small, the flow will first be expanded and then recompressed before exiting to the suction side. Hofer et al. (Ref. 7) conducted an experimental study of leakage flow for a non-rotating linear turbine cascade. The study looked at the impact of cooling in the tip gap for two squealer geometries. They considered a full squealer tip and a suction side squealer tip and concluded that the suction side squealer resulted in higher heat transfer and loss coefficient, $Y = \frac{P_{01} - P_{02}}{P_{01} - P_2}$. This

is to be expected because at subsonic conditions, the suction side squealer tip effectively acts as a converging nozzle that accelerates flow through the tip. Hofer et al. (Ref. 7) state that neglecting the relative casing motion does not significantly alter the results citing previous studies like that of Krishnababu et al. (Ref. 8). The latter studied the effect of relative casing motion on tip heat transfer and tip leakage mass flow for two different tip gap heights. They concluded that the effect of relative casing motion is diminished for larger tip gap heights due to dominant inviscid effects. In the present study, the flow is dominated by inviscid effects owing to the high Mach number.

More recently, Wheeler et al. (Ref. 9) conducted a steady CFD simulation of tip flow for a transonic turbine rotor using the Spalart-Allmaras and the standard $k-\epsilon$ turbulence (with wall function) models. They state that at high speeds, the choice of turbulence model has little effect on heat transfer prediction. Using a quasi-3D approach, they observed a quicker reattachment of the separation bubble at higher Mach number. They also state that there is a drop in heat transfer coefficient due to decreased turbulent mixing at high Mach numbers and that the flow is dominated by local pressure gradients. As it is pointed out by Wheeler et al. (Ref. 9), high speed flow through the tip gap chokes the flow and therefore provides an opportunity to move toward higher stage loading without added tip losses.

Shyam et al. (Refs. 10 and 11) performed a three-dimensional unsteady simulation of a high pressure turbine stage and analyzed the flow in the tip region. The supersonic region of the tip was found to exhibit two-dimensional, laminar flow. Bands of high and low heat flux were observed corresponding to shocks and expansions. The separation bubble that forms at the pressure side lip acts as a converging diverging nozzle for the flow through the tip gap. The reattachment of the separation bubble is accompanied by increased heat flux. A throat (minimum available flow area) was formed near the tip gap entrance at the location of maximum separation bubble height, δ . The pressure ratio across the tip was sufficiently high to make the flow sonic at the throat. The expanding tip gap (due to the separation bubble reattachment) makes the flow supersonic. The flow was observed to be over-expanded and goes through a series of shocks and expansions before the flow reaches the pressure of the suction side. Two regions of tip flow were identified. The aft 70 percent of the tip was found to be fully supersonic while the leading edge region of the tip was found to be subsonic. The work discussed in this paper deals with the aft 70 percent region where the flow is fully supersonic and choked. The flow in this region exhibits two-dimensionality and is only unsteady in a quantitative sense. Shyam et al. (Ref. 11) show that the unsteadiness results in a “hot spot” in the aft 70 percent on the tip caused by radial unsteadiness. However, the pattern of heat flux on the tip surface remains unchanged. It was suggested in Reference 11 that by contouring the tip geometry it would be possible to minimize tip heat flux without changing the tip leakage massflow due to the tip gap being choked. This study examines 5 different tip gap geometries in an attempt to reduce tip heat flux and to obtain a flat heat flux profile across the tip without increasing aerodynamic losses or tip leakage. The latter is fairly straightforward because the tip is choked. The region of the blade tip analyzed in this paper is shown in Figure 1. The range of width to height ratios is 6.0 to 2.0 for the particular geometry of (Refs. 10 and 11). The results of this study are applicable to blades experiencing regions of supersonic flow across the tip.

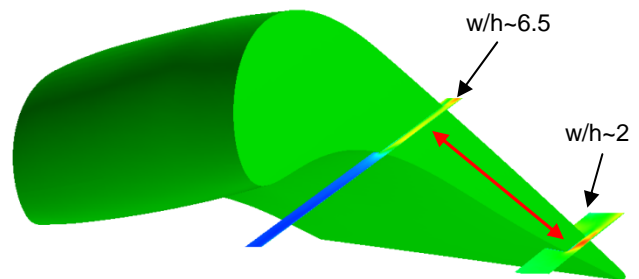


Figure 1.—Extent of supersonic tip study (denoted by red arrow).

Numerical Setup

The simulations presented in this paper were performed using the Reynolds-Averaged Navier-Stokes code GlennHT (Ref. 5). The code has previously been used to study tip heat transfer and loss (Refs. 13 and 14). A flat tip was considered the baseline case for this exercise. The flow properties were obtained from a three-dimensional CFD simulation (Ref. 10). The flow in the region of the rotor tip examined shows minimal three-dimensionality and the strong pressure gradient minimizes the impact of turbulence (Refs. 9 and 11). In this study a two-dimensional section of the tip is considered and the flow is assumed to be laminar. The results from the baseline case were compared to the three-dimensional model to ensure that the flow features were qualitatively similar. The approximate location of the two-dimensional study with respect to the three-dimensional study of (Refs. 10 and 11) is shown in Figure 2. It shows a three-dimensional representation of a turbine blade and a plane that is representative of flow in the aft 70 percent of the tip region. The ratio of tip width to tip height is approximately 6.0. In the region of the tip that represents a width to height of 2.0 or greater the supersonic flow causes a reattachment of the pressure side separation bubble. The exit Mach number was approximately 1.18 for all simulations to allow for a direct comparison. This also ensures that approximately the same massflow passes through the tip for the 5 cases considered here (because the tip is choked). The solid walls (tip and casing) are modeled as isothermal with wall temperature equal to 0.7 times the reference temperature. The reference temperature is the tip inlet temperature and was obtained from the three-dimensional simulation of (Ref. 10) and is consistent with the experiment of Tallman et al. (Ref. 12). The casing was assumed to be stationary due to the relatively thin boundary layer observed in Reference 11.

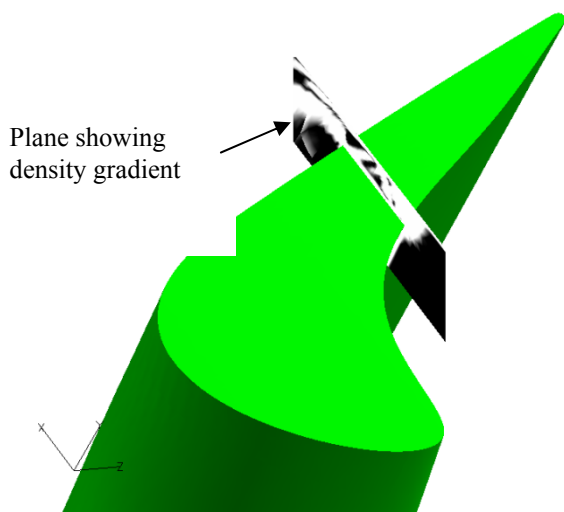


Figure 2.—Plane showing shock structure in the tip gap from three-dimensional simulation (Ref. 11).

The simulations were deemed converged when residuals achieved the value 10^{-8} and when tip surface heat flux over successive iterations was unchanged. The grids were generated using GridPro (Program Development Company) and were deemed refined based on previous studies (Refs. 9 and 11). The grid consists of approximately 70 cells in the tip to casing direction and is more refined than the grids used in References 9 and 11. The y^+ at the first cell off the wall is 0.01. Five cases are presented here although several more geometries were considered. A few of the cases that are not presented in detail here are shown in the results section with a brief description of why the design was not examined further. The results shown here are not intended to be quantitatively accurate but serve as a guideline to designing a supersonic tip.

Case 1: Baseline—Figure 3 shows the grid for the baseline case. The grid consists of approximately 81,000 cells with a majority of the cells located in the tip gap to resolve the flow. The tip gap height is $0.17w$, where w is the width of the tip and measures 0.2587 in.

Case 2: Diverging tip gap—Figure 4 shows the grid for this case. The tip gap height at the entrance to the tip gap is $0.17w$. The tip gap height at the tip exit is $0.195w$. Approximately 76000 cells were used for this case.

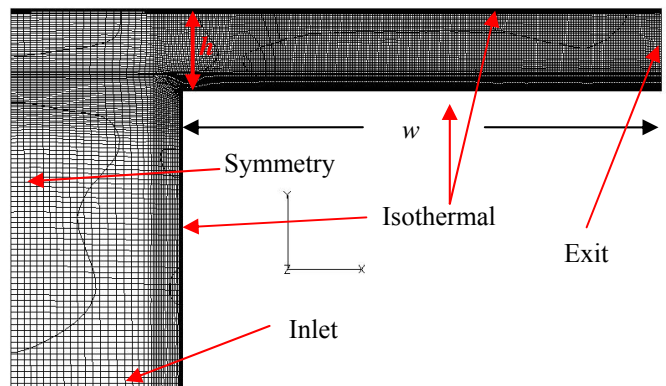


Figure 3.—Grid and boundary conditions for case 1 (flat).

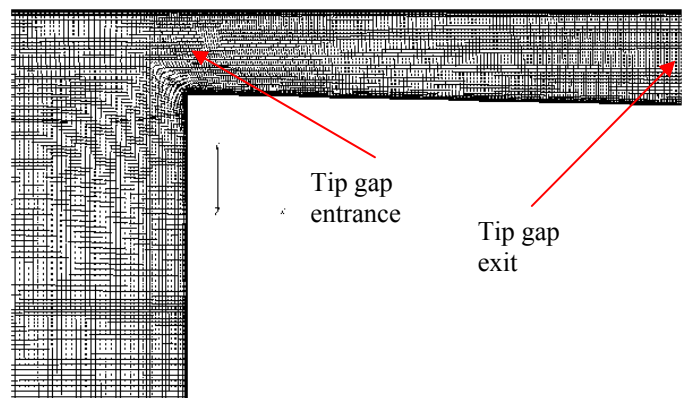


Figure 4.—Grid for case 2 (diverging).

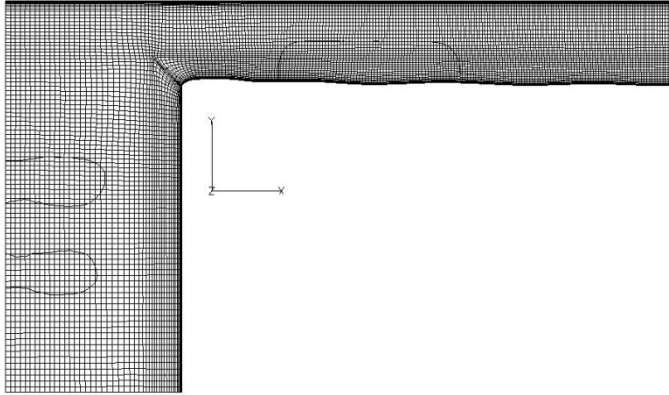


Figure 5.—Grid for case 3 (wavy wall).

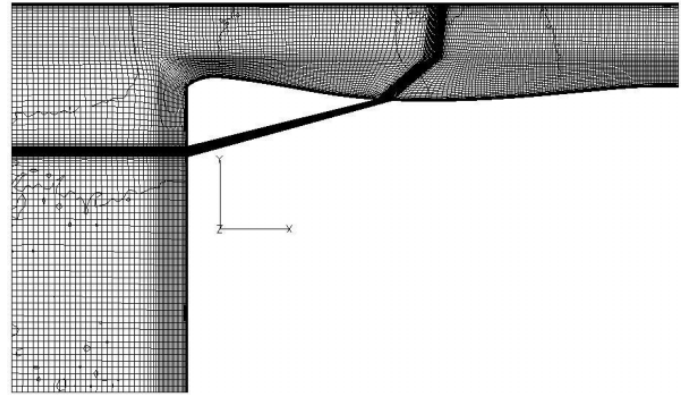


Figure 9.—Grid for case 5 (contoured tip with hole).

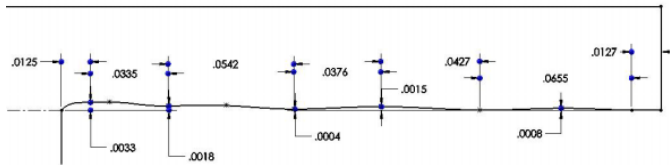


Figure 6.—Dimensions (inches) for case 3 (wavy wall).

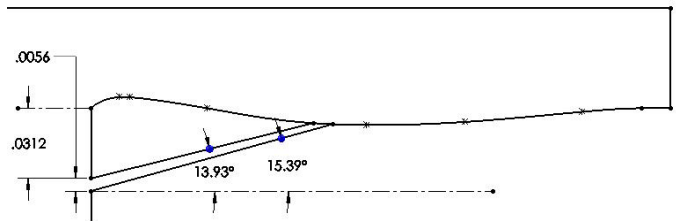


Figure 10.—Dimensions (inches) for case 5 (contoured tip with hole).

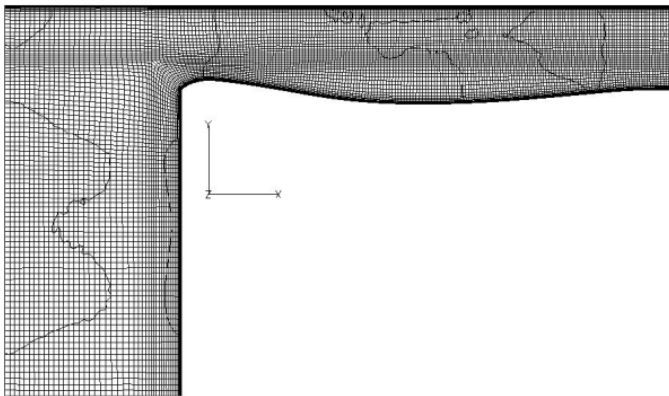


Figure 7.—Grid for case 4 (contoured tip).

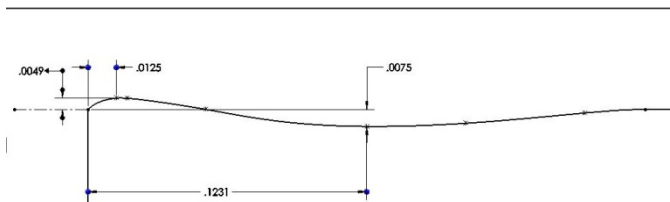


Figure 8.—Dimensions (inches) for case 4 (contoured tip).

Case 3: Wavy wall—Figure 5 shows the grid for a tip contoured as a wavy wall. The grid consists of approximately 73000 cells. The wavy wall was constructed using a spline whose control points are defined as shown in Figure 6.

Case 4: Separation-Contoured tip—Figure 7 shows the grid for the contoured tip that consists of approximately 78000 cells. The dimensions in inches of the contour are shown in Figure 8. The shape at the tip gap entrance was chosen to mimic the separation bubble at the pressure side entrance to the tip gap.

Case 5: Separation-Contoured tip with hole—The grid for case 5 is shown in Figure 9 and the dimensions in inches for the hole location are shown in Figure 10. The grid consists of approximately 106000 cells.

Results and Discussion

Flow visualization was achieved using Fieldview (Intelligent Light). Figure 10 shows the Nusselt number on the flat tip surface (case 1). The solid line represents the solution using Wilcox's $k-\omega$ turbulence model while the markers represent the laminar solution. The results of Figure 10 used a wall temperature of 0.9 times the reference temperature to make any effects of turbulence more obvious.

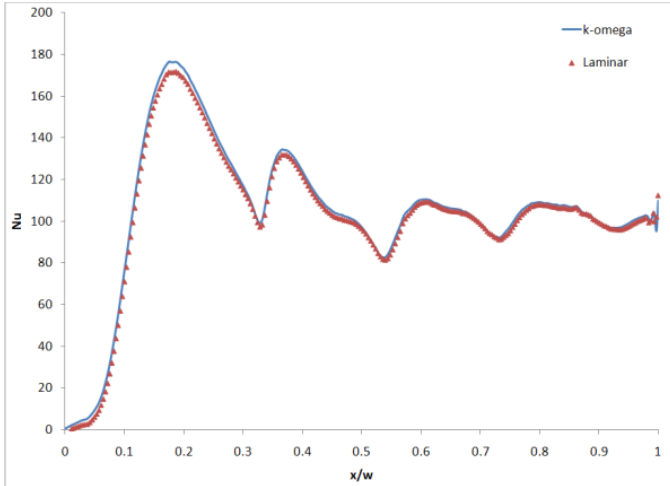


Figure 11.—Comparison of laminar solution to turbulent solution for case 1.

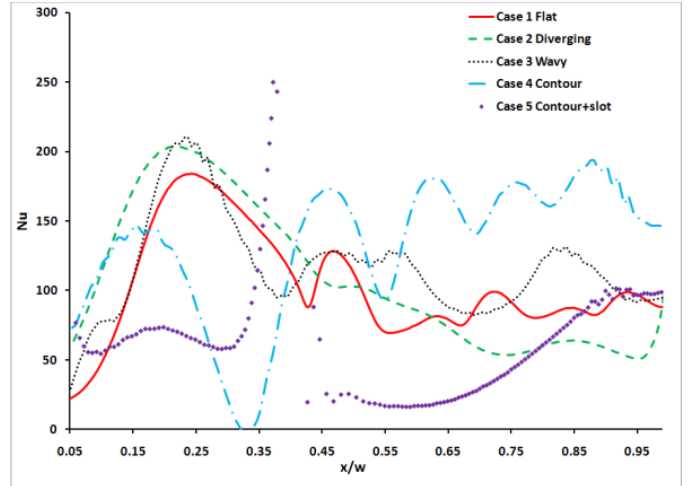


Figure 13.—Heat flux on the tip for five tip geometries.

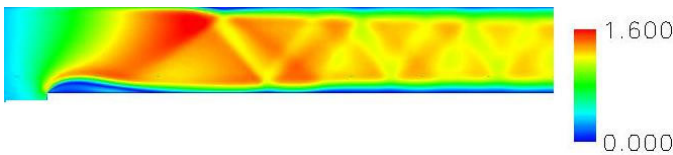


Figure 12.—Mach number contours for case 1.

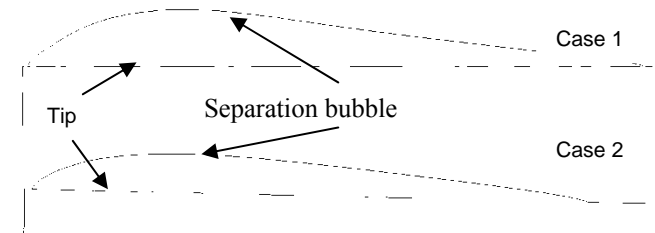


Figure 14.—Comparison of separation bubbles for cases 1 and 2.

Figure 11 shows that the effect of turbulence is negligible. With the exception of a 2 percent difference in the peak heat flux at reattachment, the pattern and magnitude of Nusselt number on the tip surface are nearly identical for the laminar and turbulent solution.

Figure 12 shows the Mach number contour for the baseline case, case 1. At the tip gap entrance the separation bubble causes a throat to form. The pressure ratio across the tip gap is sufficient to ensure that the flow at the throat is sonic. Downstream of the throat the flow expands to supersonic as explained in Reference 11. The series of shocks and expansions that ensues results in a series of peaks and valleys of high and low heat flux on the tip surface. Figure 13 shows the Nusselt number, Nu , on the tip for the five cases examined here.

The peaks and valleys are caused by the thickening and thinning of the boundary layer as the shocks and expansions interact with the boundary layer. The boundary layer itself is responsible for the shocks and expansions by causing a change in effective flow area. Therefore, if it is possible to design the tip in such a way that the boundary layer thickness and the effective flow area are approximately constant it would be possible to generate a flat heat flux profile on the tip. Furthermore, it is desirable to maintain a region of separation and a thick boundary layer to minimize the surface heat flux. In Figure 13, for case 1, the heat flux peaks at $x/w = 0.21$. This is the region of reattachment where the boundary layer is thinnest and the strong (relatively) shock forms due to the change in flow geometry. As the boundary layer thickens and the shocks decrease in strength the peak values of heat flux are

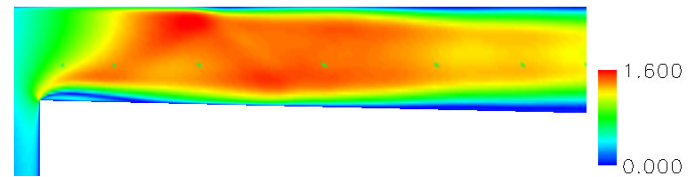


Figure 15.—Mach number contours for case 2.

reduced and the heat flux profile flattens out. Case 2 is a diverging tip gap. The idea was to gradually increase the flow area to compensate for boundary layer thickening after the first shock (most upstream location). While a thick boundary protects the tip surface it narrows the flow area in the tip gap and thus creates several shocks and reflections. By diverging the tip gap, the hope is to effectively keep the flow area constant. This would also extend the separation zone. Figure 13 shows that while downstream of the reattachment the heat flux profile is indeed “flattened”, the reattachment heating is far higher than for the baseline case.

The reason for this is that the separation bubble has been flattened as shown in Figure 14. The reattachment point is also shifted downstream. This means that the Mach number and the shock heating at reattachment are much higher. The flatter separation bubble leads to a thinner boundary layer upon reattachment and a smaller “buffer” zone under the separation bubble (Fig. 15). This is why between $x/w = 0.0$ and $x/w = 0.45$ the heat flux for case 2 is higher than the heat flux for

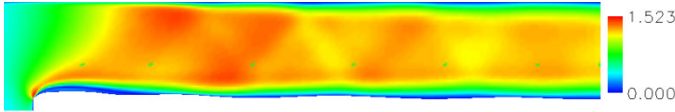


Figure 16.—Mach number contours for case 3.

case 1. Downstream of $x/w = 0.45$ the boundary layer thickens and the heat flux drops gradually and consistently towards the suction side.

Figure 15 clearly shows that the numerous shocks and expansions downstream of reattachment have been eliminated. However the region of high Mach number (red color) is still present above the separation bubble. The boundary layer (blue region) downstream of reattachment (near the tip exit) is much thicker for case 2 than for case 1.

For case 3, the wavy wall was an approximate attempt at creating valleys in the tip profile at the shock locations. This would cause the effective flow area to remain unchanged. However, because the shocks and the boundary layer feed off each other, this is a difficult task and the ideal location of the peaks and valleys for the tip contour would vary with flow conditions. Figure 13 shows that while the heat flux profile is somewhat flattened, there is still some fluctuation downstream of reattachment. Peak heat flux was also not significantly changed. The contouring of the wall does however reduce the heat flux between $x/w = 0.23$ and $x/w = 0.41$ by significantly reducing the shock strength. Peak Mach number in the tip gap is also reduced from approximately 1.6 for cases 1 and 2 to 1.52 for case 3. This can be seen in Figure 16.

Further improvement to the wavy wall design could be beneficial if the design were not so sensitive to the flow. Therefore, in case 4 a converging-diverging-converging nozzle was attempted. The entrance to the tip gap is contoured to follow the separation bubble. The idea is to eliminate separation and reattachment or to have a gentle reattachment. This objective has clearly been achieved as evidenced from Figure 13 between $x/w = 0.01$ and $x/w = 0.31$. At the tip gap entrance the flow remains attached and the heating in the $x/w = 0.01$ to $x/w = 0.31$ region is purely due to the free stream flow conditions. Unfortunately, the diverging section extends too far downstream and the flow has too far to travel through a converging section that significantly increases the surface heat flux. This is due to the extremely thin boundary layer that develops in the absence of a separated region. There are pockets of separated flow on the tip that serve to reduce heat flux but shock boundary layer interaction compensates for this decrease in heat flux. Effectively, the net heat flux downstream of $x/w = 0.40$ is raised with respect to case 1. Figure 17 shows density gradient contours for case 4. It is interesting to note the ring shaped patterns in the tip gap. These “rings” enclose a region of high pressure and low Mach number. The upstream half of the rings are compressions and similar in structure to bow shocks. The downstream half of the rings are expansions.

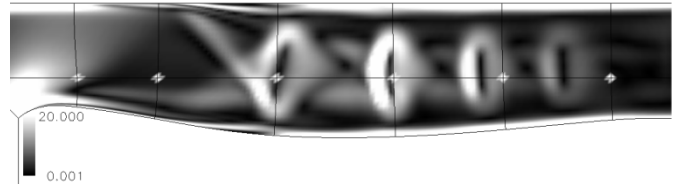


Figure 17.—Density gradient contours for case 4.

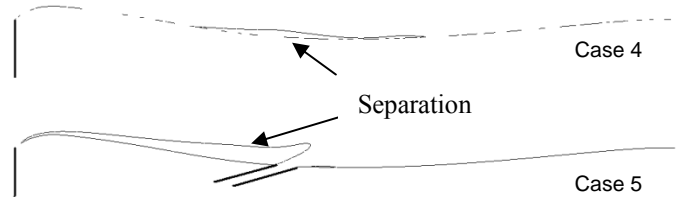


Figure 18.—Comparison of separation regions for cases 4 and 5.

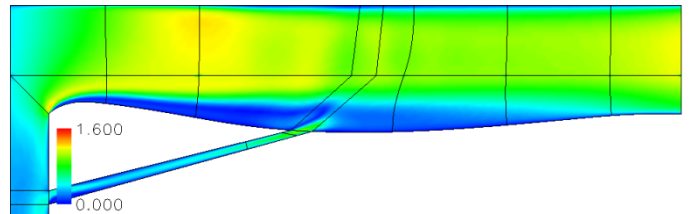


Figure 19.—Mach number contours in the tip gap for case 5.

In order to provide the benefits of both the contoured tip gap entrance (case 4) and the flat profile downstream of separation in case 2 a fifth case (case 5) was simulated that features a hole connecting the pressure side of the tip to $x/w = 0.37$ on the tip that is just upstream of the location where heat flux from case 4 is seen to exceed the heat flux from case 1. In case 5, the purpose of the hole is to add blockage to the tip gap and to energize the boundary layer downstream of $x/w = 0.37$. Figure 18 shows the separation region upstream of the hole for case 5 is markedly larger than in case 4, creating a smooth passage for the tip gap flow. Figure 19 shows the Mach number contours in the tip gap for case 5.

Figure 19 shows that the flowpath seen by the tip leakage flow is relatively smooth. The shock train is therefore almost completely eliminated leading to a lower peak Mach number and less loss. It is true that the gas jetting out through the hole is hot. However the aim of this study was to see the effect of the jet on maintaining the heat flux profile along the tip surface. The jet velocity is sufficiently high that it lifts off from the surface. Unlike in a film cooling application where this is undesirable, the jet lift off ensures that hot gas from the hole is not in prolonged contact with the tip surface downstream of injection. Future designs could ensure that the hole is encased in cooling fluid or the hole could be a cooling hole. The density ratio of the jet (ratio of density at jet exit to density at throat) is approximately 1.45. The blowing ratio (ratio of massflow per unit area at jet exit to massflow per unit area at throat) is approximately 0.65.

In either case, it is clear that the objective of energizing the boundary layer and creating an extended buffer zone is achieved with the exception of the near-hole region. In reality, the heat flux downstream of the hole could be expected to lie somewhere between that of case 1 and case 5 (shown in Fig. 10). The peak shown in Figure 13 will also probably be found to be exaggerated should an experiment be done to simulate case 5. This is an assumption based on CFD predictions of film cooling where CFD shows a sharp increase in cooling effectiveness in the near-hole region and a sudden drop to near zero effectiveness downstream. Experiments have shown that this is in fact not the case (Ref. 15). In case 5, upstream of the hole, there is a separation region that was not present in case 4. This is due to the blockage created by the jet. The net result is a lower heat flux upstream of the jet as well. Table 1 shows the cases and the improvement over the baseline case with respect to average tip heat flux and loss (by measuring entropy generation).

With the exception of case 5, the baseline case has the least aerodynamic loss. Case 3 has lower average heat flux than case 1 and has a flatter heat flux profile. Case 5 is the best design with the exception of the near hole region. Case 5 shows a 6.98 percent decrease in loss compared to the baseline case. The average heat flux for case 5 is 37.32 percent lower than for case 1 while the heat flux from case 3 is only 5.1 percent lower. As mentioned earlier, case 3 can be greatly improved by contouring the wavy wall to compliment the shock boundary layer interaction but the contouring would be very sensitive to any flow variations. Case 5 however uses the tip inlet geometry to form the throat. While there may be some fluctuation of heat flux upstream of the hole, there is a sufficient heat flux margin for case 5.

Several other configurations were also simulated that are not presented here. Figure 20 shows one such geometry purely as a caution for its unsuitability to supersonic tip flows. Over 670000 cells were used to grid this geometry due to the interesting flow visualizations seen here. The geometry is similar to a tip recess (also modeled.) The large expansion region causes extremely high Mach numbers (maximum Mach number is 2.6) and causes the flow to be unsteady due to supersonic cavity flow effects. There are severe shocks and the heat flux on the surface is several orders of magnitude higher than for the flat tip (case 1). Figures 21 and 22 show more images of the flow through the recess-like tip gap. The contours are of Mach number. Figure 21 shows the subsonic region of the flow while Figure 22 shows the supersonic region. They are separated for clarity. Other geometries that were attempted include several converging tip gap shapes. These converging tip gaps are unable to support the pressure drop across the tip gap due to the presence of the separation bubble (once the flow is sonic at the throat a converging downstream section will cause a pressure rise instead of the necessary pressure drop that is needed to achieve the suction side pressure). A conventional recess tip was also modeled and found to perform poorly.

TABLE 1.—COMPARISON OF 6 TIP GEOMETRIES

Case tip geometry	Reduction tip average heat flux	Peak Mach number	Loss improvement
	%		%
1. Flat	0.00	1.65	0.00
2. Diverging	-15.20	1.59	-39.53
3. Wavy	5.10	1.45	-1.16
4. Contoured	-39.40	1.60	-0.47
5. Hole+contour	37.32	1.27	6.98
Recess	-120.0	2.50	3.72



Figure 20.—Density gradient contours in a supersonic tip recess.

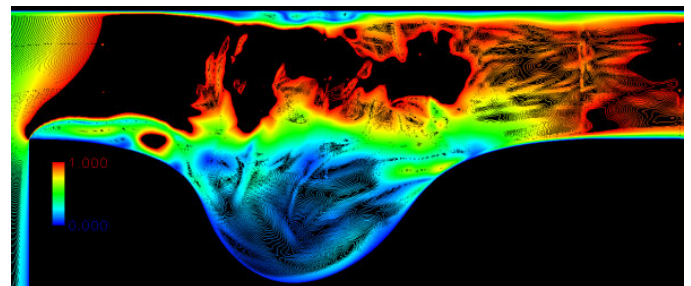


Figure 21.—Instantaneous Mach number contours in a supersonic tip recess (subsonic regime).

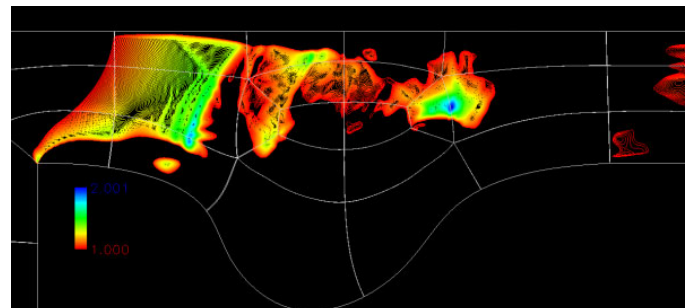


Figure 22.—Instantaneous Mach number contours in a supersonic tip recess (supersonic regime).

Conclusions

Five different two-dimensional tip geometries were simulated using the CFD code GlennHT (Ref. 5). The baseline case was a flat tip. Overall, the contoured tip geometry with a hole (case 5) had lower aerodynamic loss, lower average heat flux and a more flat heat flux profile. The shock-boundary layer interaction makes it a challenge to design tip geometry for a particular system of shocks. The ideal supersonic tip should have a nearly constant boundary layer thickness and a thick boundary layer. It has been shown that it is possible to manipulate the shock structure in the tip gap by changing the tip geometry to achieve this goal.

Future Work

In order to build on the results from the simulation of case 5 an optimizer could be used to contour the aft region of the tip to keep the boundary layer thickness fairly constant. It would also be interesting to see the effect of turbulence on the geometry of case 5 and to replace the pressure side hole with a cooling hole.

References

1. Bunker, R.S., "A Review of Turbine Blade Tip Heat Transfer," *Annals of the New York Academy of Science*, Vol. 934, pp 64-79, January 2006.
2. Glezer, B., Harvey, N.W., Camci, C., Bunker, R.S., Ameri, A.A., "Turbine Blade Tip Design and Tip Clearance Treatment," notes from von Karman Lecture Series 2004, June 2004.
3. Zhou, C., and Hodson, H., "The Tip Leakage flow of an Unshrouded High Pressure Turbine Blade With Tip Cooling," ASME-GT2009-59637, June 2009.
4. O'Dowd, D., Zhang, Q., Ligrani, P., He, L., Friedrichs, S., "Comparison of Heat Transfer Measurement Techniques on a Transonic Turbine Blade Tip," ASME-GT2009-59376, June 2009.
5. Ameri, A.A., Steinthorsson, E., Rigby, D.L., "Effect of Squealer Tip on Rotor Heat Transfer and Efficiency," *Journal of Turbomachinery*, Vol. 120, pp 753-759, October 1998.
6. Ameri, A.A., Steinthorsson, E., Rigby, D.L., "Effects of Tip Clearance and Casing Recess on Heat Transfer and Stage Efficiency in Axial Turbines," *Journal of Turbomachinery*, Vol. 121, pp 683-693, October 1999.
7. Hofer, T., Arts, T., "Aerodynamic Investigation of the Tip Leakage Flow for Blades With Different Tip Squealer Geometries at Transonic Conditions," ASME-GT2009-59909, June 2009.
8. Krishnababu, S.K., Dawes, W.N., Hodson, H.P., Lock, G.D., Hannis, J., Whitney, C., "Aero-Thermal Investigations of Tip Leakage Flow in Axial Flow Turbines, Part II -Effect of Relative Casing Motion," ASME 2007-GT-27957, May 2007.
9. Wheeler, A.P.S., Atkins, R., He, L., "Turbine Blade Tip Heat Transfer in Low and High Speed Flows," ASME-GT2009-59404, June 2009.
10. Shyam, V., Ameri, A., Luk, D.F., and Chen, J.P., "3-D Unsteady Simulation of a Modern High Pressure Turbine Stage Using Phase Lag Periodicity: Analysis of Flow and Heat Transfer," *Journal of Turbomachinery*, Vol. 133, Iss. 3, July 2011.
11. Shyam V., Ameri A., Chen J.P., "Analysis of Unsteady Tip and Endwall Heat Transfer in a Highly Loaded Transonic Turbine Stage," GT2010-23694, June 2010.
12. Tallman, J.A., Haldeman, C.W., Dunn, M.G., Tolpadi, A.K., and Bergholz, R.F., "Heat Transfer Measurements and Predictions for a Modern, High-Pressure, Transonic Turbine, Including Endwalls," ASME-GT2006-90927, May 2006.
13. Ameri, Ali A., "Heat Transfer and Flow on the Tip of a Gas Turbine Equipped With a Mean-Camberline Strip," ASME paper 2001-GT-0156, June 2001, NASA/CR—2001-210764.
14. Ameri, A.A. and Bunker, R.S., "Heat Transfer and Flow on the First Stage Blade Tip of a Power Generation Gas Turbine, Part 2: Simulation Results," ASME paper 99-GT-283, June, 1999, also NASA/CR-1999-209151, April, 1999.
15. Sinha, A.K., Bogard, D.G., and Crawford, M.E., "Film-Cooling Effectiveness Downstream of a Single Row of Holes With Variable Density Ratio," *Journal of Turbomachinery*, Vol. 113, pp 442-449, 1991.

REPORT DOCUMENTATION PAGE			Form Approved OMB No. 0704-0188		
<p>The public reporting burden for this collection of information is estimated to average 1 hour per response, including the time for reviewing instructions, searching existing data sources, gathering and maintaining the data needed, and completing and reviewing the collection of information. Send comments regarding this burden estimate or any other aspect of this collection of information, including suggestions for reducing this burden, to Department of Defense, Washington Headquarters Services, Directorate for Information Operations and Reports (0704-0188), 1215 Jefferson Davis Highway, Suite 1204, Arlington, VA 22202-4302. Respondents should be aware that notwithstanding any other provision of law, no person shall be subject to any penalty for failing to comply with a collection of information if it does not display a currently valid OMB control number.</p> <p>PLEASE DO NOT RETURN YOUR FORM TO THE ABOVE ADDRESS.</p>					
1. REPORT DATE (DD-MM-YYYY) 01-07-2012		2. REPORT TYPE Technical Memorandum		3. DATES COVERED (From - To)	
4. TITLE AND SUBTITLE Comparison of Various Supersonic Turbine Tip Designs to Minimize Aerodynamic Loss and Tip Heating			5a. CONTRACT NUMBER		
			5b. GRANT NUMBER		
			5c. PROGRAM ELEMENT NUMBER		
6. AUTHOR(S) Shyam, Vikram; Ameri, Ali			5d. PROJECT NUMBER		
			5e. TASK NUMBER		
			5f. WORK UNIT NUMBER WBS 561581.02.08.03.21.14.03		
7. PERFORMING ORGANIZATION NAME(S) AND ADDRESS(ES) National Aeronautics and Space Administration John H. Glenn Research Center at Lewis Field Cleveland, Ohio 44135-3191			8. PERFORMING ORGANIZATION REPORT NUMBER E-18188		
9. SPONSORING/MONITORING AGENCY NAME(S) AND ADDRESS(ES) National Aeronautics and Space Administration Washington, DC 20546-0001			10. SPONSORING/MONITOR'S ACRONYM(S) NASA		
			11. SPONSORING/MONITORING REPORT NUMBER NASA/TM-2012-217607		
12. DISTRIBUTION/AVAILABILITY STATEMENT Unclassified-Unlimited Subject Categories: 02, 34, and 07 Available electronically at http://www.sti.nasa.gov This publication is available from the NASA Center for AeroSpace Information, 443-757-5802					
13. SUPPLEMENTARY NOTES					
14. ABSTRACT The rotor tips of axial turbines experience high heat flux and are the cause of aerodynamic losses due to tip clearance flows, and in the case of supersonic tips, shocks. As stage loadings increase, the flow in the tip gap approaches and exceeds sonic conditions. This introduces effects such as shock-boundary layer interactions and choked flow that are not observed for subsonic tip flows that have been studied extensively in literature. This work simulates the tip clearance flow for a flat tip, a diverging tip gap and several contoured tips to assess the possibility of minimizing tip heat flux while maintaining a constant massflow from the pressure side to the suction side of the rotor, through the tip clearance. The Computational Fluid Dynamics (CFD) code GlennHT was used for the simulations. Due to the strong favorable pressure gradients the simulations assumed laminar conditions in the tip gap. The nominal tip gap width to height ratio for this study is 6.0. The Reynolds number of the flow is 2.4×10^5 based on nominal tip width and exit velocity. A wavy wall design was found to reduce heat flux by 5 percent but suffered from an additional 6 percent in aerodynamic loss coefficient. Conventional tip recesses are found to perform far worse than a flat tip due to severe shock heating. Overall, the baseline flat tip was the second best performer. A diverging converging tip gap with a hole was found to be the best choice. Average tip heat flux was reduced by 37 percent and aerodynamic losses were cut by over 6 percent.					
15. SUBJECT TERMS Supersonic heat transfer; Supersonic turbine; Supersonic flow blade tips					
16. SECURITY CLASSIFICATION OF:			17. LIMITATION OF ABSTRACT	18. NUMBER OF PAGES 14	19a. NAME OF RESPONSIBLE PERSON STI Help Desk (email:help@sti.nasa.gov)
a. REPORT U	b. ABSTRACT U	c. THIS PAGE U			UU

